arXiv:1403.0096v1 [hep-ph] 1 Mar 2014

Octet negative parity to octet positive parity electromagnetic transitions in light cone QCD

T. M. Aliev *†, M. Savcı ‡

Physics Department, Middle East Technical University, 06531 Ankara, Turkey

Abstract

Light cone QCD sum rules for the electromagnetic transition form factors among positive and negative parity octet baryons are derived. The unwanted contributions of the diagonal transitions among positive parity octet baryons are eliminated by combining the sum rules derived from different Lorentz structures. The Q^2 dependence for the transversal and longitudinal helicity amplitudes are studied.

PACS numbers: 11.55.Hx, 13.40.Gp, 14.20.Gk

*taliev@metu.edu.tr

†Permanent address: Institute of Physics, Baku, Azerbaijan.

‡savci@metu.edu.tr

1 Introduction

According to the quark-gluon picture baryons are represented as their bound states, and for this reason what is measured in experiments is actually indirect manifestation of their realizations. The experimental investigation for obtaining information about the internal structure of baryons is based on measurement of the form factors. One main direction in getting useful information in order to understand the internal structure of baryons is to study the electromagnetic properties of the baryons. At present, except the proton and neutron, the electromagnetic form factors of octet spin-1/2 baryons have not yet been studied experimentally.

The experiments conducted at Jefferson Laboratory (JLab) and Mainz Microton facilty play the key role in study of the electromagnetic structure of baryons via the scattering of electrons on nucleons, i.e., $eN \to eN^*$, where N^* is the nucleon excitation. These reactions proceed through the $\gamma^* N \to N^*$, where γ^* is the virtual photon, and these transitions are described by the electromagnetic form factors. The study of the properties of nucleon excitations, in particular the form factors constitute one of the main research programs of the above-mentioned laboratories.

In one of our previous works we analyzed the $\gamma^* N \to N^*(1535)$ transition form factors [1] within the light cone QCD sum rules method (LCSR) [2] (for an application of the LCSR on baryon form factors, see also [3]). The experiments that have been conducted at JLab for this experiment have collected a lot of data. The future planned experiments at JLab will allow the chance to study the structure of N^* at high photon virtualities up to $Q^2 = 12\ GeV^2$ (see [4]). This transition has already been studied in framework of the covariant quark model [5] and lattice gauge theory [6].

In the present work we extend our previous work for the $\gamma^* N \to N^*(1535)$ transition [1] to all members of the positive and negative parity spin-1/2 octet baryons. In this regard we analyze the $\gamma^*\Sigma \to \Sigma^*$ and $\gamma^*\Xi \to \Xi^*$ transitions and calculate their transition form factors within framework of the LCSR. All these transitions are customarily denoted as $\gamma^* B \to B^*$, where B represents the spin-1/2 positive parity; and B^* represents the spin-1/2 negative parity baryons.

The paper is organized in the following way. In section 2, the sum rules for the form factors of the $\gamma^* B \to B^*$ transitions are derived in LCSR. Section 3 is devoted to the numerical analysis, summary and conclusions.

2 Transition form factors of $\gamma^* B \to B^*$

It is well known that in describing the $\gamma^* B \to B^*$ transition, the electromagnetic current J_μ^{el} is sandwiched between B with momentum p and B^* with momentum p', i.e., $\left\langle B^*(p') \left| J_\mu^{el}(q) \right| B(p) \right\rangle$. This matrix element is parametrized in terms of two form factors as:

$$\left\langle B^*(p') \left| J_\mu^{el}(q) \right| B(p) \right\rangle = \bar{u}_{B^*}(p') \Bigg[\left(\gamma_\mu - \frac{\not{q} q_\mu}{q^2} \right) F_1^*(Q^2) - \frac{i}{m_B + m_{B^*}} \sigma_{\mu\nu} q^\nu F_2^*(Q^2) \Bigg] \gamma_5 u_B(p) \ , \tag{1}$$

where $F_1^*(Q^2)$; and $F_2^*(Q^2)$ are the Dirac and Pauli form factors, respectively; $q = p - p'$; and $Q^2 = -q^2$. Appearance of the second term in F_1^* is dictated by the conservation of the electromagnetic current. In order to derive the LCSR for the form factors $F_1^*(Q^2)$ and $F_2^*(Q^2)$ we consider the following vacuum-to-ground state positive parity baryon correlation function:

$$\Pi_\alpha(p,q) = i \int d^4x e^{iqx} \left\langle 0 \left| \mathcal{T}\{\eta(0) J_\alpha^{el}(x)\} \right| B(p) \right\rangle \ . \tag{2}$$

Here η is the interpolating current of the octet baryon, and $J_\alpha^{el}(x) = e_u \bar{u}\gamma_\alpha u + e_d \bar{d}\gamma_\alpha d + e_s \bar{s}\gamma_\alpha s$ is the electromagnetic current. The general form of the interpolating currents for light octet baryons are given as:

$$\begin{aligned}
\eta_{\Sigma^+} &= 2\varepsilon^{abc} \sum_{\ell=1}^{2} (u^{aT} C A_1^\ell s^b) A_2^\ell u^c \ , \\
\eta_{\Sigma^-} &= \eta_{\Sigma^+}(u \to d) \ , \\
\eta_{\Sigma^0} &= \sqrt{2}\varepsilon^{abc} \sum_{\ell=1}^{2} \left[(u^{aT} C A_1^\ell s^b) A_2^\ell d^c + (d^{aT} C A_1^\ell s^b) A_2^\ell u^c \right] \ , \\
\eta_{\Xi^0} &= \eta_{\Sigma^+}(u \leftrightarrow s) \ , \\
\eta_{\Xi^-} &= \eta_{\Sigma^-}(d \leftrightarrow s) \ ,
\end{aligned} \tag{3}$$

where C is the charge conjugation operator; and $A_1^1 = I$; $A_1^2 = A_2^1 = \gamma_5$; and $A_2^2 = \beta$.

We consider now the hadronic transitions involving negative parity baryons. According to the standard procedure for obtaining sum rules for the corresponding physical quantities, we substitute in Eq. (1) the total set of negative and positive parity baryon states between the interpolating and electromagnetic currents. The resulting hadronic dispersion relations contain contributions from the lowest positive parity baryon and its negative parity partner. The matrix element of the interpolating current between the vacuum and one-particle positive parity baryon states is determined as:

$$\langle 0 \left| \eta \right| B(p) \rangle = \lambda_B u_B(p) \ , \tag{4}$$

where λ_B is the residue of the corresponding baryon. Similarly, the matrix element of the interpolating current between the vacuum and one-particle negative parity baryon states is defined as:

$$\langle 0 \left| \eta \right| B^*(p) \rangle = \lambda_{B^*} \gamma_5 u_{B^*}(p) \ . \tag{5}$$

The hadronic matrix elements $\left\langle B(p-q) \left| J_\alpha^{el} \right| B(p) \right\rangle$ and $\left\langle B^*(p-q) \left| J_\alpha^{el} \right| B(p) \right\rangle$ are defined in terms of the form factors. The second of these matrix elements which is written in terms of the Dirac and Pauli type form factors is given in Eq. (1). The first matrix element describing the electromagnetic transition among positive parity baryons can be obtained from Eq. (1) by making the following replacements $F_{1,2}^*(Q^2) \to F_{1,2}(Q^2)$, and then omitting the $\not{q} q_\alpha / q^2$ terms and replacing γ_5 with the unit matrix.

Using the equation of motion $(\not{p} - m_B)u_B(p) = 0$, the correlation function can be represented in terms of six independent invariant functions as:

$$\Pi_\alpha((p-q)^2, q^2) = \Pi_1((p-q)^2, q^2)\gamma_\alpha + \Pi_2((p-q)^2, q^2)q_\alpha + \Pi_3((p-q)^2, q^2)q_\alpha \not{q} + \Pi_4((p-q)^2, q^2)p_\alpha + \Pi_5((p-q)^2, q^2)p_\alpha \not{q} + \Pi_6((p-q)^2, q^2)\gamma_\alpha \not{q} \ , \quad (6)$$

where all invariant functions depend on $(p-q)^2$ and q^2.

Using the definition of the form factors and residues, and performing summation over the baryon spin we get the following expressions for the invariant functions:

$$\begin{aligned}
\Pi_1((p-q)^2, q^2) &= -\frac{\lambda_{B^*}(m_{B^*} + m_B)}{m_{B^*}^2 - (p-q)^2} F_1^*(q^2) - \frac{\lambda_{B^*}(m_{B^*} - m_B)}{m_{B^*}^2 - (p-q)^2} F_2^*(q^2) + \cdots \\
\Pi_2((p-q)^2, q^2) &= \frac{\lambda_{B^*}(m_{B^*}^2 - m_B^2)}{q^2[m_{B^*}^2 - (p-q)^2]} F_1^*(q^2) + \frac{\lambda_{B^*}(m_{B^*} - m_B)}{(m_{B^*} + m_B)[m_{B^*}^2 - (p-q)^2]} F_2^*(q^2) \\
&+ \frac{\lambda_B}{m_B^2 - (p-q)^2} F_2(q^2) + \cdots \\
\Pi_3((p-q)^2, q^2) &= \frac{\lambda_{B^*}(m_{B^*} + m_B)}{q^2[m_{B^*}^2 - p'^2]} F_1^*(q^2) + \frac{\lambda_{B^*}}{(m_{B^*} + m_B)[m_{B^*}^2 - (p-q)^2]} F_2^*(q^2) \\
&- \frac{\lambda_B}{2m_B[m_B^2 - (p-q)^2]} F_2(q^2) + \cdots
\end{aligned} \quad (7)$$

Here dots correspond to the contributions of the excited and continuum states with quantum numbers of B and B^*. According to the quark hadron duality these contributions are modeled as perturbative ones starting on from some threshold s_0.

Employing the nucleon interpolating current, we now calculate the correlation function from the QCD side. In order to justify the expansion of the product of two current near the light cone $x^2 \simeq 0$, the external momenta are taken in deep Eucledian domain. The operator product expansion (OPE) is carried out over twist which involves the distribution amplitudes (DAs) of the baryon with growing twist. The matrix element of the three quark operators between the vacuum and the state of the members of the positive parity octet baryons is defined in terms of the DAs of the baryons, i.e.,

$$\varepsilon^{abc} \left\langle 0 \left| q_{1\alpha}^a(a_1 x) q_{2\beta}^b(a_2 x) q_{3\gamma}^c(a_3 x) \right| B(p) \right\rangle \ , \quad (8)$$

where a, b, c are the color indices; a_1, a_2; and a_3 are positive numbers.

Using the Lorentz covariance, and parity and spin of the baryons this matrix element can be written in terms of 27 DAs as:

$$4\varepsilon^{abc} \left\langle 0 \left| q_{1\alpha}^a(a_1 x) q_{2\beta}^b(a_2 x) q_{3\gamma}^c(a_3 x) \right| B(p) \right\rangle = \sum_i \mathcal{F}_i \Gamma_{\alpha\beta}^{1i} \left[\Gamma^{2i} B(p) \right]_\gamma \ , \quad (9)$$

where Γ^i are certain Dirac matrices; and $\mathcal{F}_i$ are the DAs which do not posses definite twist. For completeness, the matrix element (9) is presented in Appendix A.

The matrix element given in Eq. (8) is defined in terms of the definite twist DAs as:

$$4\varepsilon^{abc} \left\langle 0 \left| q_{1\alpha}^a(a_1 x) q_{2\beta}^b(a_2 x) q_{3\gamma}^c(a_3 x) \right| B(p) \right\rangle = \sum_i F_i \Gamma_{\alpha\beta}^{\prime 1i} \left[\Gamma^{\prime 2i} B(p) \right]_\gamma \ ,$$

and the two sets of DAs are connected to each other by the following relations:

$$
\begin{array}{ll}
\mathcal{S}_1 = S_1 \ , & (2P\cdot x)\,\mathcal{S}_2 = S_1 - S_2 \ , \\
\mathcal{P}_1 = P_1 \ , & (2P\cdot x)\,\mathcal{P}_2 = P_2 - P_1 \ , \\
\mathcal{V}_1 = V_1 \ , & (2P\cdot x)\,\mathcal{V}_2 = V_1 - V_2 - V_3 \ , \\
2\mathcal{V}_3 = V_3 \ , & (4P\cdot x)\,\mathcal{V}_4 = -2V_1 + V_3 + V_4 + 2V_5 \ , \\
(4P\cdot x)\,\mathcal{V}_5 = V_4 - V_3 \ , & (2P\cdot x)^2\,\mathcal{V}_6 = -V_1 + V_2 + V_3 + V_4 + V_5 - V_6 \ , \\
\mathcal{A}_1 = A_1 \ , & (2P\cdot x)\,\mathcal{A}_2 = -A_1 + A_2 - A_3 \ , \\
2\mathcal{A}_3 = A_3 \ , & (4P\cdot x)\,\mathcal{A}_4 = -2A_1 - A_3 - A_4 + 2A_5 \ , \\
(4P\cdot x)\,\mathcal{A}_5 = A_3 - A_4 \ , & (2P\cdot x)^2\,\mathcal{A}_6 = A_1 - A_2 + A_3 + A_4 - A_5 + A_6 \ , \\
\mathcal{T}_1 = T_1 \ , & (2P\cdot x)\,\mathcal{T}_2 = T_1 + T_2 - 2T_3 \ , \\
2\mathcal{T}_3 = T_7 \ , & (2P\cdot x)\,\mathcal{T}_4 = T_1 - T_2 - 2T_7 \ , \\
(2P\cdot x)\,\mathcal{T}_5 = -T_1 + T_5 + 2T_8 \ , & (2P\cdot x)^2\,\mathcal{T}_6 = 2T_2 - 2T_3 - 2T_4 + 2T_5 + 2T_7 + 2T_8 \ , \\
(4P\cdot x)\,\mathcal{T}_7 = T_7 - T_8 \ , & (2P\cdot x)^2\,\mathcal{T}_8 = -T_1 + T_2 + T_5 - T_6 + 2T_7 + 2T_8 \ .
\end{array}
\tag{10}
$$

We also present the explicit expressions of the DAs with definite twist in Appendix B.

The calculation of the invariant amplitudes from the QCD side is tedious but straightforward. The invariant amplitudes in terms of the spectral densities ρ_{2i}, ρ_{4i}, and ρ_{6i} can be written as:

$$
\Pi_i = N \int_0^1 dx \left\{ \frac{\rho_{2i}(x)}{(q-px)^2} + \frac{\rho_{4i}(x)}{(q-px)^4} + \frac{\rho_{6i}(x)}{(q-px)^6} \right\} \ , \tag{11}
$$

where $N = 2$ for the Σ^+, Σ^-, Ξ^0, and Ξ^-; and $\sqrt{2}$ for Σ^0 baryons. Explicit expressions of the spectral densities ρ_{2i}, ρ_{4i}, and ρ_{6i} are presented in Appendix C. It should be noted that the sum rules derived from combinations of different Lorentz structures are suggested in [7].

Equating Eqs. (7) and (11), and performing Borel transformation over $-(p-q)^2$ we get the following sum rules for the $\gamma^* B \to B^*$ transition form factors:

$$
\begin{aligned}
\lambda_{B^*} \left[m_{B^*} + m_B) F_1^*(Q^2) + m_{B^*} - m_B) F_2^*(Q^2) \right] e^{-m_{B^*}^2/M^2} &= -I_1(Q^2, M^2, s_0) \ , \\
\lambda_{B^*} \left[-\frac{m_{B^*} + m_B)}{Q^2} F_1^*(Q^2) + F_2^*(Q^2) \right] e^{-m_{B^*}^2/M^2} &= -I_1(Q^2, M^2, s_0) \\
&\quad + 2 m_B I_3(Q^2, M^2, s_0) \ ,
\end{aligned}
\tag{12}
$$

and $I_i(Q^2, M^2, s_0)$ are determined to be:

$$
\begin{aligned}
I_i(Q^2, M^2, s_0) = \int_{x_0}^1 dx \Bigg[& - \frac{\rho_{2i}(x)}{x} + \frac{\rho_{4i}(x)}{x^2 M^2} - - \frac{\rho_{6i}(x)}{2x^3 M^4} \Bigg] e^{-s(x)/M^2} \\
& + \Bigg[\frac{\rho_{4i}(x_0)}{Q^2 + x_0^2 m_B^2} - \frac{1}{2x_0} \frac{\rho_{6i}(x_0)}{(Q^2 + x_0^2 m_B^2) M^2} \\
& + \frac{1}{2} \frac{x_0^2}{(Q^2 + x_0^2 m_B^2)} \left(\frac{d}{dx_0} \frac{\rho_{6i}(x_0)}{x_0 (Q^2 + x_0^2 m_B^2) M^2} \right) \Bigg] e^{-s_0/M^2} \Bigg\} \ ,
\end{aligned}
\tag{13}
$$

where

$$
s(x) = \frac{\bar{x} Q^2 + x \bar{x} m_B^2}{x} \ ,
$$

and x_0 is the solution of $s(x) = s_0$.

As has already been noted, the analysis of the experimental data for the nucleon system is performed with the Dirac and Pauli type form factors. The data for the nucleon resonances is mostly analyzed with the help of helicity amplitudes (see for example [4, 8, 9]). In other words, in the analysis of data related to the negative parity baryons it is more suitable to study the helicity amplitudes instead of Dirac and Pauli type form factors. The electro production of negative parity spin-1/2 baryon resonance in the $\gamma^* B \to B^*$ transitions is described with the help of two independent, transverse amplitude $A_{1/2}$ and longitudinal amplitude $S_{1/2}$. The relations among the form factors F_1^* and F_2^*, and helicity amplitudes $A_{1/2}$ and $S_{1/2}$ is given as:

$$A_{1/2} = -2e\sqrt{\frac{(m_{B^*}+m_B)^2+Q^2}{8m_B(m_{B^*}^2-m_B^2)}}\left[F_1^*(Q^2)+\frac{m_{B^*}-m_B}{m_{B^*}+m_B}F_2^*(Q^2)\right] , \tag{14}$$

$$S_{1/2} = \sqrt{2}e\sqrt{\frac{(m_{B^*}+m_B)^2+Q^2}{8m_B(m_{B^*}^2-m_B^2)}}\frac{|\vec{q}|}{Q^2}\left[\frac{m_{B^*}-m_B}{m_{B^*}+m_B}F_1^*(Q^2) - \frac{Q^2}{(m_{B^*}+m_B)^2}F_2^*(Q^2)\right] , \tag{15}$$

where e is the electric charge; and $\vec{q}$ is the photon three-momentum whose absolute value in the rest frame of B^* is given as:

$$|\vec{q}| = \frac{\sqrt{Q^4+2Q^2(m_{B^*}^2+m_B^2)+(m_{B^*}^2-m_B^2)^2}}{2m_{B^*}} .$$

In determining the form factors F_1^* and F_2^* from the sum rules given in Eq. (12) the residues λ_{B^*} of the negative parity baryons are needed, which is obtained from the two-point correlation function

$$\Pi(p^2) = i\int d^4x e^{ipx}\left\langle 0\left|\mathrm{T}\left\{\eta(x)\bar{\eta}(0)\right\}\right|0\right\rangle .$$

Following the same procedure presented in [1], we get for the mass and residue of the negative parity spin-1/2 octet baryons

$$m_{B^*}^2 = \frac{\int_0^{s_0} ds\, e^{-s/M^2} s\Big[m_B\mathrm{Im}\Pi_1(s)-\mathrm{Im}\Pi_2(s)\Big]}{\int_0^{s_0} ds\, e^{-s/M^2}\Big[m_B\mathrm{Im}\Pi_1(s)-\mathrm{Im}\Pi_2(s)\Big]} , \tag{16}$$

$$|\lambda_{B^*}|^2 = \frac{e^{m_{B^*}^2/M^2}}{m_{B^*}+m_B}\frac{1}{\pi}\int_0^{s_0} ds\, e^{-s/M^2}\Big[m_B\mathrm{Im}\Pi_1(s)-\mathrm{Im}\Pi_2(s)\Big] , \tag{17}$$

$\mathrm{Im}\Pi_1(s)$ and $\mathrm{Im}\Pi_2(s)$ correspond to the spectral densities for the $\not{p}$ and unit operator structures, respectively, and they are calculated in [10].

3 Numerical analysis

In the previous section we have calculated the $\gamma^* B \to B^*$ transition form factors and helicity amplitudes using within the framework of the LCSR method. In this section we will present our numerical results on the helicity amplitudes.

The main nonperturbative contributions to LCSR are realized by the DAs, which are presented in the Appendix. In the numerical analysis we will use the DAs of the Σ, Ξ and λ baryons which are calculated in [11–13]. The parameters appearing in the expressions of the DAs are determined from the two-point QCD sum rules, and their values are given as:

$$\begin{aligned}
f_\Xi &= (9.9 \pm 0.4) \times 10^{-3}\ GeV^2\ , \\
\lambda_1 &= -(2.1 \pm 0.1) \times 10^{-2}\ GeV^2\ , \\
\lambda_2 &= (5.2 \pm 0.2) \times 10^{-2}\ GeV^2\ , \\
\lambda_3 &= (1.7 \pm 0.1) \times 10^{-2}\ GeV^2\ ,
\end{aligned}$$

$$\begin{aligned}
f_\Sigma &= (9.4 \pm 0.4) \times 10^{-3}\ GeV^2\ , \\
\lambda_1 &= -(2.5 \pm 0.1) \times 10^{-2}\ GeV^2\ , \\
\lambda_2 &= (4.4 \pm 0.1) \times 10^{-2}\ GeV^2\ , \\
\lambda_3 &= (2.0 \pm 0.1) \times 10^{-2}\ GeV^2\ ,
\end{aligned} \tag{18}$$

We have recalculated these parameters once more and obtained that the sum rules of these parameters given in [9–11] contain errors. Our reanalysis on these parameters predicts that:

$$\begin{aligned}
f_\Xi &= (11.70 \pm 0.4) \times 10^{-3}\ GeV^2\ , \\
\lambda_1 &= -(3.15 \pm 0.1) \times 10^{-2}\ GeV^2\ , \\
\lambda_2 &= (6.50 \pm 0.2) \times 10^{-2}\ GeV^2\ , \\
\lambda_3 &= (2.15 \pm 0.1) \times 10^{-2}\ GeV^2\ ,
\end{aligned}$$

$$\begin{aligned}
f_\Sigma &= (13.00 \pm 0.4) \times 10^{-3}\ GeV^2\ , \\
\lambda_1 &= -(3.15 \pm 0.1) \times 10^{-2}\ GeV^2\ , \\
\lambda_2 &= (6.75 \pm 0.1) \times 10^{-2}\ GeV^2\ , \\
\lambda_3 &= (1.80 \pm 0.1) \times 10^{-2}\ GeV^2\ ,
\end{aligned} \tag{19}$$

which we shall use in our numerical analysis. The masses of the negative parity baryons are taken from the QCD sum rules estimation give in Eq. (17) having the values: $m_{\Sigma^*} = (1.7 \pm 0.1)\ GeV$ $m_{\Xi^*} = (1.75 \pm 0.1)\ GeV$, and $m_{\Lambda^*} = (1.7 \pm 0.1)\ GeV$ which are very close to the experimental results. For the quark condensate we use $\langle \bar{q} q \rangle (1\ GeV) = -\left(246^{+28}_{-19}\ MeV\right)^3$ [14].

The domain of the Borel mass parameter used in the calculations for the form factors is chosen to be $M^2 = (1.8 \pm 0.4)\ GeV^2$, which is decided with the criteria that the power and continuum contributions are sufficiently suppressed. The value of the continuum threshold is determined in such a way that the mass sum rules prediction reproduce the experimentally measured mass to within the limits of 10-15% accuracy, and this condition leads that

$s_0 = (3.7 \pm 0.3)\ GeV^2$. The working region of the arbitrary parameter β is determined from the condition that $\lambda^2_{B^*}$ be positive and exhibit good stability with respect to the variation in β. Our analysis shows that the residues of all negative parity baryons satisfy the above-required conditions in the range $0.4 \leq \beta \leq 0.8$, which we shall use in further numerical analysis.

In Figs. (1) and (2) we depict the photon momentum square Q^2 dependence of the helicity amplitudes $A_{1/2}$ and $S_{1/2}$ for the $\gamma^*\Sigma^+ \to \Sigma^{+*}$, respectively, at $M^2 = 1.6\ GeV^2$, $s_0 = 3.5\ GeV^2$, and at three fixed values of β picked from its working region. For the parameters λ_1, λ_2 and λ_3 appearing in DAs, we use our own results given in Eq. (19). In order to keep higher twist, continuum and higher states contributions under control Q^2 is restricted vary in the domain $1\ GeV^2 \leq Q^2 \leq 10\ GeV^2$. It follows from Fig. (1) that, $A_{1/2}$ decreases with increasing Q^2 and tends to zero asymptotically. The situation for $S_{1/2}$ is presented in Fig. (2), from which we observe that it also mimics the behavior of $A_{1/2}$ and tends to zero at large Q^2. We see that the transversal helicity amplitude is 3 to 4 times smaller in modulo compared to the longitudinal helicity amplitude $S_{1/2}$ at all values of Q^2.

In Figs. (3) and (4) the dependencies of $A_{1/2}$ and $S_{1/2}$ on Q^2 at the same values of M^2 and s_0 are presented for the $\gamma^*\Sigma^- \to \Sigma^{-*}$ transition, respectively. The trends in regard to their dependence on Q^2 are same, i.e., both amplitudes decrease with increasing Q^2 in modulo. We also observe that the values of the modulo of $A_{1/2}$ and $S_{1/2}$ are small compared to the $\gamma^*\Sigma^+ \to \Sigma^{+*}$ transition, at least 2 to 3 times.

In Figs. (5) and (6) we present the Q^2 dependence of the transversal and longitudinal helicity amplitudes for the $\gamma^*\Sigma^0 \to \Sigma^{0*}$ transition. We see from these figures that the magnitude of $A_{1/2}$ seems to be slightly smaller compared to the $\gamma^*\Sigma^- \to \Sigma^{-*}$ case, while the magnitude of $S_{1/2}$ appears to be approximately 50% larger compared to the same transition.

The Q^2 dependence of $A_{1/2}$ and $S_{1/2}$ for the $\gamma^*\Xi^- \to \Xi^{-*}$ transition are given in Figs. (7) and (8). We observe from these figures that the values of $A_{1/2}$ are quite similar to the ones predicted for the $\gamma^*\Sigma^- \to \Sigma^{-*}$ transition. In the case of $S_{1/2}$ however, the difference between the transitions is around 40%.

Finally, Figs. (9) and (10) depict the dependence of the helicity amplitudes on Q^2 for the $\gamma^*\Xi^0 \to \Xi^{0*}$ transition. It follows from these figures that, $A_{1/2}$ change its sign at $Q^2 = 1.5\ GeV^2$ at the fixed value of the arbitrary parameter $\beta = 0.8$. The maximum value $A_{1/2}$ is equal to 0.04 at $Q^2 = 1\ GeV^2$, when $\beta = 0.4$. We further see that the magnitude of $S_{1/2}$ is quite close to the one predicted for the $\gamma^*\Sigma^0 \to \Sigma^{0*}$ transition.

We can summarize our results as follows:

- The transversal helicity amplitude $A_{1/2}$ seems to be practically insensitive to the values of the arbitrary parameter β for the $\gamma^*\Sigma^- \to \Sigma^{-*}$ and $\gamma^*\Xi^- \to \Xi^{-*}$ transitions.

- Contrary to the above behavior, the same amplitude $A_{1/2}$ for the $\gamma^*\Sigma^+ \to \Sigma^{+*}$ is quite sensitive to the value of β. The value of $A_{1/2}$ at $Q^2 = 1\ GeV^2$ doubles itself when β changes from 0.4 to 0.8.

- The longitudinal amplitude $S_{1/2}$ does weakly depend on β for all considered transitions.

Of course measurement of these electromagnetic form factors is quite difficult due to the short life-time of hyperons. We hope that along with further developments in experimental techniques, measurement of these transition form factors could become possible.

It should be noted here that, our results can be improved further with the help of more reliable calculations of DAs and with the inclusion of perturbative $\mathcal{O}(\alpha_s)$ corrections, and the first attempt in this direction has already been made in [15].

In conclusion, we investigate the electromagnetic transition among octet positive and negative parity baryons within LCSR method. We calculate the transversal and longitudinal helicity amplitudes described by these transitions. The Q^2 dependence of these amplitudes are studied. We show that the longitudinal helicity amplitude seems to be practically insensitive to the variations in the arbitrary parameter β for all considered transitions.

References

[1] T. M. Aliev, M. Savcı, Phys. Rev. D **88**, 056021 (2013).

[2] V. M. Braun, arXiv:9801222 [hep-ph].

[3] A. Lenz, M. Gockeler, T. Kaltenbrunner, and N. Warkentin, Phys. Rev. D **79**, 093007 (2009).

[4] I. G. Aznauryan *et. al*, Int. J. Mod. Phys. E **22**, 1330015 (2013).

[5] G. Ramalho, Phys. Rev. D **84**, 033007 (2011).

[6] Huey-Wen Lin, S. D. Cohen, R. G. Edwards, and D. G. Richards, Phys. Rev. D **78**, 114508 (2008).

[7] A. Khodjamirian, C. Klein, T. Mannel, and Y. M. Wang, J. High Energy Phys. **1109**, 106 (2011).

[8] C. F. Perdrisat, V. Punjabi, and M. Vanderhaeghen, Prog. Part. Nucl. Phys. **59**, 694 (2007).

[9] G. Ramalho, and K. Tsushima, Phys. Rev. D **84**, 051301 (2011).

[10] T. M. Aliev, A. Özpineci, M. Savci, Phys. Rev. D **66**, 016002 (2002).

[11] Y.-L. Liu, M.-Q. Huang, Nucl.Phys. A **821**, 80 (2009).

[12] Y.-L. Liu, M.-Q. Huang, Phys. Rev. D **79**, 114031 (2009); *ibid* D **80**, 055015 (2009).

[13] Y.-L. Liu, M.-Q. Huang, J. Phys. G **37**, 115010 (2010).

[14] G. Duplancic, A. Khodjamirian, Th. Mannel, B. Melic, and N. Offen, J. High Energy Phys. **0804**, 014 (2008).

[15] I. V. Anikin, V. M. Braun, and N. Offen, Phys. Rev. D **88**, 114021 (2013).

[16] V. M. Braun, A. Lenz, M. Wittmann, Phys. Rev. D **73**, 094019 (2006).

Appendix A

In this appendix we present the general Lorentz decomposition of the matrix element of the three-quark operators between the vacuum and the octet baryon states in terms of the DAs [16].

$$
\begin{aligned}
4\left\langle 0\left|\varepsilon^{ijk}u^i_\alpha(a_1x)u^j_\beta(a_2x)d^k_\gamma(a_3x)\right|B(p)\right\rangle = \\
&\mathcal{S}_1 m_B C_{\alpha\beta}\left(\gamma_5 B\right)_\gamma + \mathcal{S}_2 m_B^2 C_{\alpha\beta}\left(\not{x}\gamma_5 B\right)_\gamma + \mathcal{P}_1 m_B\left(\gamma_5 C\right)_{\alpha\beta} B_\gamma + \mathcal{P}_2 m_B^2\left(\gamma_5 C\right)_{\alpha\beta}\left(\not{x} B\right)_\gamma \\
+ &\left(\mathcal{V}_1 + \frac{x^2 m_B^2}{4}\mathcal{V}_1^M\right)\left(\not{p} C\right)_{\alpha\beta}\left(\gamma_5 B\right)_\gamma + \mathcal{V}_2 m_B\left(\not{p} C\right)_{\alpha\beta}\left(\not{x}\gamma_5 B\right)_\gamma + \mathcal{V}_3 m_B\left(\gamma_\mu C\right)_{\alpha\beta}\left(\gamma^\mu\gamma_5 B\right)_\gamma \\
+ &\mathcal{V}_4 m_B^2\left(\not{x} C\right)_{\alpha\beta}\left(\gamma_5 B\right)_\gamma + \mathcal{V}_5 m_B^2\left(\gamma_\mu C\right)_{\alpha\beta}\left(i\sigma^{\mu\nu}x_\nu\gamma_5 B\right)_\gamma + \mathcal{V}_6 m_B^3\left(\not{x} C\right)_{\alpha\beta}\left(\not{x}\gamma_5 B\right)_\gamma \\
+ &\left(\mathcal{A}_1 + \frac{x^2 m_B^2}{4}\mathcal{A}_1^M\right)\left(\not{p}\gamma_5 C\right)_{\alpha\beta} B_\gamma + \mathcal{A}_2 m_B\left(\not{p}\gamma_5 C\right)_{\alpha\beta}\left(\not{x} B\right)_\gamma + \mathcal{A}_3 m_B\left(\gamma_\mu\gamma_5 C\right)_{\alpha\beta}\left(\gamma^\mu B\right)_\gamma \\
+ &\mathcal{A}_4 m_B^2\left(\not{x}\gamma_5 C\right)_{\alpha\beta} B_\gamma + \mathcal{A}_5 m_B^2\left(\gamma_\mu\gamma_5 C\right)_{\alpha\beta}\left(i\sigma^{\mu\nu}x_\nu B\right)_\gamma + \mathcal{A}_6 m_B^3\left(\not{x}\gamma_5 C\right)_{\alpha\beta}\left(\not{x} B\right)_\gamma \\
+ &\left(\mathcal{T}_1 + \frac{x^2 m_B^2}{4}\mathcal{T}_1^M\right)\left(p^\nu i\sigma_{\mu\nu} C\right)_{\alpha\beta}\left(\gamma^\mu\gamma_5 B\right)_\gamma + \mathcal{T}_2 m_B\left(x^\mu p^\nu i\sigma_{\mu\nu} C\right)_{\alpha\beta}\left(\gamma_5 B\right)_\gamma \\
+ &\mathcal{T}_3 m_B\left(\sigma_{\mu\nu} C\right)_{\alpha\beta}\left(\sigma^{\mu\nu}\gamma_5 B\right)_\gamma + \mathcal{T}_4 m_B\left(p^\nu\sigma_{\mu\nu} C\right)_{\alpha\beta}\left(\sigma^{\mu\rho}x_\rho\gamma_5 B\right)_\gamma \\
+ &\mathcal{T}_5 m_B^2\left(x^\nu i\sigma_{\mu\nu} C\right)_{\alpha\beta}\left(\gamma^\mu\gamma_5 B\right)_\gamma + \mathcal{T}_6 m_B^2\left(x^\mu p^\nu i\sigma_{\mu\nu} C\right)_{\alpha\beta}\left(\not{x}\gamma_5 B\right)_\gamma \\
+ &\mathcal{T}_7 m_B^2\left(\sigma_{\mu\nu} C\right)_{\alpha\beta}\left(\sigma^{\mu\nu}\not{x}\gamma_5 B\right)_\gamma + \mathcal{T}_8 m_B^3\left(x^\nu\sigma_{\mu\nu} C\right)_{\alpha\beta}\left(\sigma^{\mu\rho}x_\rho\gamma_5 B\right)_\gamma \ ,
\end{aligned}
$$

where C is the charge conjugation operator; and B represents the octet baryon with momentum p.

Appendix B

twist-4 DAs:

$$
\begin{aligned}
V_2(x_i) &= 24x_1x_2[\phi_4^0 + \phi_4^+(1-5x_3)] \ , \\
A_2(x_i) &= 24x_1x_2(x_2-x_1)\phi_4^- \ , \\
T_2(x_i) &= 24x_1x_2[\xi_4^0 + \xi_4^+(1-5x_3)] \ , \\
V_3(x_i) &= 12x_3\{\psi_4^0(1-x_3) + \psi_4^+(1-x_3-10x_1x_2) + \psi_4^-[x_1^2+x_2^2-x_3(1-x_3)]\} \ , \\
A_3(x_i) &= 12x_3(x_2-x_1)[(\psi_4^0+\psi_4^+) + \psi_4^-(1-2x_3)] \ , \\
T_3(x_i) &= 6x_3\{B(\phi_4^0+\psi_4^0+\xi_4^0)(1-x_3) + (\phi_4^++\psi_4^++\xi_4^+)(1-x_3-10x_1x_2) \\
&\quad + (\phi_4^--\psi_4^-+\xi_4^-)[x_1^2+x_2^2-x_3(1-x_3)]\} \ , \\
T_7(x_i) &= 6x_3\{(\phi_4^0+\psi_4^0-\xi_4^0)(1-x_3) + (\phi_4^++\psi_4^+-\xi_4^+)(1-x_3-10x_1x_2) \\
&\quad + (\phi_4^--\psi_4^--\xi_4^-)[x_1^2+x_2^2-x_3(1-x_3)]\} \ , \\
S_1(x_i) &= 6x_3(x_2-x_1)[(\phi_4^0+\psi_4^0+\xi_4^0+\phi_4^++\psi_4^++\xi_4^+) + (\phi_4^--\psi_4^-+\xi_4^-)(1-2x_3)] \ , \\
P_1(x_i) &= 6x_3(x_1-x_2)[(\phi_4^0+\psi_4^0-\xi_4^0+\phi_4^++\psi_4^+-\xi_4^+) + (\phi_4^--\psi_4^--\xi_4^-)(1-2x_3)] \ ,
\end{aligned}
$$

twist-5 DAs:

$$
\begin{aligned}
V_4(x_i) &= 3\{\psi_5^0(1-x_3) + \psi_5^+[1-x_3-2(x_1^2+x_2^2)] + \psi_5^-[2x_1x_2-x_3(1-x_3)]\} \ , \\
A_4(x_i) &= 3(x_2-x_1)[-\psi_5^0 + \psi_5^+(1-2x_3) + \psi_5^-x_3] \ , \\
T_4(x_i) &= \frac{3}{2}\{(\phi_5^0+\psi_5^0+\xi_5^0)(1-x_3) + (\phi_5^++\psi_5^++\xi_5^+)[1-x_3-2(x_1^2+x_2^2)]\} \\
&\quad + (\phi_5^--\psi_5^-+\xi_5^-)[2x_1x_2-x_3(1-x_3)] \ , \\
T_8(x_i) &= \frac{3}{2}\{(\phi_5^0+\psi_5^0-\xi_5^0)(1-x_3) + (\phi_5^++\psi_5^+-\xi_5^+)[1-x_3-2(x_1^2+x_2^2)] \\
&\quad + (\phi_5^--\psi_5^-+\xi_5^-)[2x_1x_2-x_3(1-x_3)]\} \ , \\
V_5(x_i) &= 6x_3[\phi_5^0 + \phi_5^+(1-2x_3)] \ , \\
A_5(x_i) &= 6x_3(x_2-x_1)\phi_5^- \ , \\
T_5(x_i) &= 6x_3[\xi_5^0 + \xi_5^+(1-2x_3)] \ , \\
S_2(x_i) &= \frac{3}{2}(x_2-x_1)[-(\phi_5^0+\psi_5^0+\xi_5^0) + (\phi_5^++\psi_5^++\xi_5^+)(1-2x_3) \\
&\quad + (\phi_5^--\psi_5^-+\xi_5^-)x_3] \ , \\
P_2(x_i) &= \frac{3}{2}(x_1-x_2)[-(\phi_5^0+\psi_5^0-\xi_5^0) + (\phi_5^++\psi_5^+-\xi_5^+)(1-2x_3) \\
&\quad + (\phi_5^--\psi_5^--\xi_5^-)x_3] \ ,
\end{aligned}
$$

twist-6 DAs:

$$
V_6(x_i) = 2[\phi_6^0 + \phi_6^+(1-3x_3)] \ ,
$$

$$A_6(x_i) = 2(x_2 - x_1)\phi_6^- \ ,$$
$$T_6(x_i) = 2[\phi_6^0 - \frac{1}{2}(\phi_6^+ - \phi_6^-)(1 - 3x_3) \ .$$

Appendix C

In this appendix we present the expressions for the functions ρ_{2i}, ρ_{4i} and ρ_{6i} which appear in the sum rules for $F_i^*(Q^2)$ for the $\gamma^*\Sigma^+ \to \Sigma^{*+}$ transition.

$$
\begin{aligned}
\rho_{61}^{\Sigma^{*+}}(x) &= e_u m_B^3 Q^2 \frac{(Q^2+m_B^2x^2)}{x}\Big[4(m_{B^*}-m_B)(1+\beta)(2-x)+m_u(1-\beta)x\Big]\,\breve{\breve{B}}_6(x)\\
&+ e_u m_u m_B^2 Q^2\Big\{4m_B^2(m_{B^*}-m_B)(1+\beta)(2-x)\Big(\widetilde{\widetilde{C}}_6+\widetilde{\widetilde{D}}_6\Big)\\
&+ \frac{(1-\beta)}{x}\Big[m_B^2[8m_{B^*}-m_B(8-x^2)]x\,\widetilde{\widetilde{B}}_6+Q^2[4m_{B^*}-m_B(4-x)]\,\widetilde{\widetilde{B}}_6\\
&- 8m_B^2(m_{B^*}-m_B)x(2-x)\,\widetilde{\widetilde{B}}_8\Big]\Big\}(x)\\
&+ e_s m_B^2\frac{Q^2}{x}\Big\{4m_s m_B^2(m_{B^*}-m_B)(1-\beta)(2-x)x\Big(\widehat{\widehat{C}}_6-\widehat{\widehat{D}}_6\Big)\\
&+ 4(1+\beta)m_B(m_{B^*}-m_B)(2-x)\Big[2m_s m_B x\,\widehat{\widehat{B}}_8+(Q^2+m_B^2x^2)\,\widehat{\widehat{B}}_6\Big]\\
&+ (1+\beta)m_s\Big[xm_B^2[8m_{B^*}-m_B(8-x^2)]+Q^2[4m_{B^*}-m_B(4-x)]\Big]\,\widehat{\widehat{B}}_6\Big\}(x)
\end{aligned}
$$

$$
\begin{aligned}
\rho_{41}^{\Sigma^{*+}}(x) &= \frac{1}{2}e_u m_B^3 Q^2(1-\beta)\Big\{2\,[2m_{B^*}-m_B(2-x)]\,\Big(\check{\check{C}}_6+\check{\check{D}}_6\Big)+m_u\,\check{\check{B}}_6\Big\}(x)\\
&- e_u m_B^3\frac{Q^2}{x}(1+\beta)\Big\{\Big[m_B[8-(5-x)x]-m_{B^*}(8-5x)\Big]\,\check{\check{B}}_6\\
&- 3x[2m_{B^*}-m_B(2-x)]\,\check{\check{B}}_8\Big\}(x)\\
&+ e_u m_B^2\frac{Q^2}{2x}(1-\beta)\Big\{2m_B x[2m_{B^*}-m_B(2-x)]\Big(\widetilde{\widetilde{C}}_6-\widetilde{\widetilde{D}}_6\Big)\\
&- m_u\Big[m_B(8+x)\,\widetilde{\widetilde{B}}_6-8m_{B^*}\,\widetilde{\widetilde{B}}_6-4m_B x\,\widetilde{\widetilde{B}}_8\Big]\Big\}(x)\\
&+ e_u m_B^2\frac{Q^2}{2x}(1+\beta)\Big\{Q^2\,\widetilde{\widetilde{B}}_6-m_B x[m_B x+4(m_{B^*}-m_B)]\Big(\widetilde{\widetilde{B}}_6-2\,\widetilde{\widetilde{B}}_8\Big)\\
&- 2m_u m_B x\Big(\widetilde{\widetilde{C}}_6+\widetilde{\widetilde{D}}_6\Big)\Big\}(x)\\
&- e_s m_B^3 Q^2(1-\beta)\Big[m_B x\Big(\widehat{\widehat{C}}_6+\widehat{\widehat{D}}_6\Big)+m_s\Big(\widehat{\widehat{C}}_6-\widehat{\widehat{D}}_6\Big)\Big](x)\\
&+ e_s m_B^2\frac{Q^2}{2x}(1+\beta)\Big\{2m_B x[2(m_s+m_{B^*})-m_B(2+x)]\,\widehat{\widehat{B}}_8\\
&+ \Big[2m_B(m_{B^*}-m_B)(8-3x)-2Q^2+m_s[8m_{B^*}-m_B(8+x)]\Big]\,\widehat{\widehat{B}}_6\Big\}(x)\\
&- e_u m_B\frac{Q^2}{2x}(1-\beta)\Big\{2m_B(x^3m_B^2-2Q^2)\Big(\check{C}_2+\check{D}_2\Big)\\
&+ 2m_B x\Big[2m_B(m_{B^*}-m_B)\Big(2\check{C}_2+\check{C}_4-3\check{C}_5+2\check{D}_2-\check{D}_4+3\check{D}_5\Big)+Q^2\Big(\check{C}_2+\check{D}_2\Big)\Big]\\
&+ Q^2\Big[4m_{B^*}\Big(\check{C}_2+\check{D}_2\Big)+m_u\Big(\check{B}_2+5\check{B}_4\Big)\Big]
\end{aligned}
$$

$$
\begin{aligned}
&- m_B^2 x^2\Big[2(m_{B^*}-m_B)\Big(\check{C}_4-3\check{C}_5-\check{D}_4+3\check{D}_5\Big)\\
&+ m_u\Big(\check{B}_2-\check{B}_4+6\check{B}_5+12\check{B}_7-2\check{E}_1+2\check{H}_1\Big)\Big]\Big\}(x)\\
&+ e_u m_B\frac{Q^2}{2x}(1+\beta)\Big\{-[2(m_{B^*}-m_B)Q^2+m_B^3x^3]\Big(\check{B}_2+5\check{B}_4\Big)\\
&+ 2m_B^2(m_{B^*}-m_B)x^2\Big(\check{B}_2-\check{B}_4+6\check{B}_5+12\check{B}_7-2\check{E}_1+2\check{H}_1\Big)\\
&+ m_B x\Big[-Q^2\Big(\check{B}_2+5\check{B}_4\Big)-8m_B(m_{B^*}-m_B)\Big(\check{B}_2+2\check{B}_4+3\check{B}_5+6\check{B}_7-\check{E}_1+\check{H}_1\Big)\\
&+ m_u\Big[m_B^2x^2\Big(\check{C}_4-3\check{C}_5-\check{B}_4+3\check{B}_5\Big)-Q^2\Big(\check{C}_2+\check{D}_2\Big)\Big]\Big\}(x)\\
&- e_u m_B\frac{Q^2}{2x}(1-\beta)\Big\{2m_B^2(m_{B^*}-m_B)(2-x)x\Big(\widetilde{C}_4-\widetilde{C}_5+\widetilde{D}_4-\widetilde{D}_5\Big)\\
&+ m_u\Big[Q^2\Big(\widetilde{B}_2+\widetilde{B}_4\Big)+4m_B(m_{B^*}-m_B)x\Big(\widetilde{B}_2-\widetilde{B}_4+2\widetilde{B}_5\Big)\\
&- m_B^2x\Big(\widetilde{B}_2-\widetilde{B}_4+2\widetilde{B}_5+2\widetilde{E}_1+2\widetilde{H}_1\Big)\Big]\Big\}(x)\\
&+ e_u m_B\frac{Q^2}{2x}(1+\beta)\Big\{-[4(m_{B^*}-m_B)Q^2+m_B^3x^3]\Big(\widetilde{B}_2+\widetilde{B}_4\Big)\\
&+ 8m_B^2(m_{B^*}-m_B)x^2\Big(\widetilde{B}_5+2\widetilde{B}_7\Big)+m_B x\Big[-Q^2\Big(\widetilde{B}_2+\widetilde{B}_4\Big)\\
&- 8m_B(m_{B^*}-m_B)\Big(\widetilde{B}_2+\widetilde{B}_4+2\widetilde{B}_5+4\widetilde{B}_7\Big)\Big]\\
&+ m_u\Big[-m_B x[2m_{B^*}-m_B(2-x)]\Big(\widetilde{C}_4-\widetilde{D}_4\Big)\\
&+ m_B x[2m_{B^*}-m_B(2+x)]\Big(\widetilde{C}_5-\widetilde{D}_5\Big)+2Q^2\Big(\widetilde{C}_2+\widetilde{D}_2\Big)\Big]\Big\}(x)\\
&- e_s m_B\frac{Q^2}{2x}(1-\beta)\Big\{4(m_{\mathcal{O}^*}-m_B)(2m_B^2x+Q^2)\Big(\widehat{C}_2+\widehat{D}_2\Big)\\
&- 4m_B^2(m_{B^*}-m_B)(2-x)x\Big(\widehat{C}_5-\widehat{D}_5\Big)+m_s\Big[-2Q^2\Big(\widehat{C}_2-\widehat{D}_2\Big)\\
&+ m_B x[2m_{B^*}-m_B(2-x)]\Big(\widehat{C}_4+\widehat{D}_4\Big)+m_B x[2m_{B^*}-m_B(2+x)]\Big(\widehat{C}_5+\widehat{D}_5\Big)\Big]\Big\}(x)\\
&+ e_s m_B\frac{Q^2}{2x}(1+\beta)\Big\{2(m_{B^*}-m_B)Q^2\Big(\widehat{B}_2-3\widehat{B}_4\Big)+m_B^3x^3\Big(\widehat{B}_2+\widehat{B}_4\Big)\\
&+ 2m_B^2(m_{B^*}-m_B)x^2\Big(\widehat{B}_2-\widehat{B}_4+2\widehat{B}_5+4\widehat{B}_7-2\widehat{E}_1+2\widehat{H}_1\Big)\\
&+ m_B x\Big[Q^2\Big(\widehat{B}_2+\widehat{B}_4\Big)-8m_B(m_{B^*}-m_B)\Big(\widehat{B}_4+\widehat{B}_5+2\widehat{B}_7-2\widehat{E}_1+\widehat{H}_1\Big)\Big]\\
&- m_s\Big[Q^2\Big(\widehat{B}_2+\widehat{B}_4\Big)-m_B^2x^2\Big(\widehat{B}_2-\widehat{B}_4+2\widehat{B}_5-2\widehat{E}_1-2\widehat{H}_1\Big)\\
&- 4m_B(m_{B^*}-m_B)x\Big(\widehat{B}_2-\widehat{B}_4+2\widehat{B}_5\Big)\Big]\Big\}(x)\\
&- e_u m_B^3[2m_{B^*}-m_B(2-x)]Q^2\int_0^{\bar{x}}dx_3\Big[(1-\beta)(A_1^M-V_1^M)-3(1+\beta)T_1^M\Big](x,1-x-x_3,x_3)\\
&+ e_u m_B^2\frac{Q^2}{x}\int_0^{\bar{x}}dx_1\Big\{(1-\beta)Q^2(A_1^M+V_1^M)
\end{aligned}
$$

$$
\begin{aligned}
&+ m_B x(1+\beta)[4m_{B^*} - m_B(4-x)]T_1^M\Big\}(x_1, x, 1-x_1-x) \\
&+ e_s m_B^2 Q^2 \int_0^{\bar{x}} dx_1 \Big\{[2m_B(m_B - m_{B^*})x - Q^2](1-\beta)(A_1^M - V_1^M) \\
&+ m_B x[2m_{B^*} - m_B(2+x)](1+\beta)T_1^M\Big\}(x_1, 1-x_1-x, x)
\end{aligned}
$$

$$
\begin{aligned}
\rho_{21}^{\Sigma^{*+}}(x) &= e_u m_B^2 \frac{Q^2}{2x}(1+\beta)\,\widetilde{\widetilde{B}}_6(x) \\
&- e_s m_B^2 \frac{Q^2}{x}(1+\beta)\,\widehat{\widehat{B}}_6(x) \\
&- e_u m_B \frac{Q^2}{2x}\Big\{(1+\beta)\Big[(m_{B^*} - m_B)\Big(\check{B}_2 + 5\check{B}_4\Big) + m_u\Big(\check{C}_2 + \check{D}_2\Big)\Big] \\
&+ (1-\beta)\Big[4(m_{B^*} - m_B)\Big(\check{B}_2 + \check{B}_4\Big) + m_u\Big(\check{B}_2 + 5\check{B}_4\Big)\Big]\Big\}(x) \\
&+ e_u m_B \frac{Q^2}{2x}\Big\{2(1+\beta)\Big[-2(m_{B^*} - m_B)\Big(\widetilde{B}_2 + \widetilde{B}_4\Big) \\
&+ m_B x\Big(\widetilde{B}_4 + \widetilde{B}_5 + 2\widetilde{B}_7 + \widetilde{E}_1 - \widetilde{H}_1\Big) + m_u\Big(\widetilde{C}_2 + \widetilde{D}_2\Big)\Big] \\
&+ (1-\beta)\Big[2m_B x\Big(\widetilde{C}_2 - \widetilde{C}_5 - \widetilde{D}_2 - \widetilde{D}_5\Big) - m_u\Big(\widetilde{B}_2 + \widetilde{B}_4\Big)\Big]\Big\}(x) \\
&- e_s m_B \frac{Q^2}{2x}\Big\{(1-\beta)\Big[4(m_{B^*} - m_B)\Big(\widehat{C}_2 - \widehat{D}_2\Big) - m_B x\Big(\widehat{C}_4 - \widehat{C}_5 - \widehat{D}_4 + \widehat{D}_5\Big) \\
&- 2m_s\Big(\widehat{C}_2 - \widehat{D}_2\Big)\Big] - (1+\beta)\Big[2m_{B^*}\Big(\widehat{B}_2 - 3\widehat{B}_4\Big) - 2m_B(1-x)\widehat{B}_2 + 6m_B\widehat{B}_4 \\
&+ 2m_B x\Big(\widehat{B}_4 + 2\widehat{B}_5 + 4\widehat{B}_7\Big) - m_s\Big(\widehat{B}_2 + \widehat{B}_4\Big)\Big]\Big\}(x) \\
&+ e_u m_B Q^2\{[2m_{B^*} - m_B(2-x)](1+\beta) + m_u(1-\beta)\} \\
&\times \int_0^{\bar{x}} dx_3\,(P_1 + S_1 + 3T_1 - 6T_3)(x, 1-x-x_3, x_3) \\
&- e_u m_B Q^2\{[2m_{B^*} - m_B(2-x)](1-\beta) + m_u(1+\beta)\} \\
&\times \int_0^{\bar{x}} dx_3\,(A_1 + 2A_3 - V_1 + 2V_3)(x, 1-x-x_3, x_3) \\
&+ e_u m_B Q^2(1+\beta)\int_0^{\bar{x}} dx_1\,\Big[4(m_{B^*} - m_B)(T_1 - 2T_3) + m_B x(P_1 + S_1 + T_1 - 2T_3) \\
&+ m_u(A_1 + A_3 - V_1 + V_3)\Big](x_1, x, 1-x_1-x) \\
&+ e_u m_B \frac{Q^2}{x}(1-\beta)\int_0^{\bar{x}} dx_1\,\Big[m_B^2 A_1^M + 2m_B(m_{B^*} - m_B)x(A_3 - V_3) + Q^2(A_1 + V_1) \\
&+ m_u m_B x(P_1 - S_1 + T_1)\Big](x_1, x, 1-x_1-x) \\
&- e_s m_B Q^2(1+\beta)\int_0^{\bar{x}} dx_1\,\Big\{m_B\Big[(2-x)(P_1 + S_1) + (2+x)(T_1 - 2T_3)\Big] \\
&- 2m_{B^*}(P_1 + S_1 + T_1 - 2T_3) + m_s(P_1 - S_1 - T_1)\Big\}(x_1, 1-x_1-x, x)
\end{aligned}
$$

$$
\begin{aligned}
&- e_s\frac{Q^2}{x}(1-\beta)\int_0^{\bar{x}} dx_1\Big\{m_B x\Big[2m_{B^*}(A_1+A_3-V_1+V_3)+m_s(A_1+A_3+V_1-V_3)\Big]\\
&- Q^2(A_1-V_1)-m_B^2\Big[(A_1^M-V_1^M)+2x(A_1+A_3-V_1+V_3)\Big]\Big\}(x_1,1-x_1-x,x)
\end{aligned}
$$

$$
\begin{aligned}
\rho_{62}^{\Sigma^{*+}}(x) &= -e_u m_B^3\frac{(Q^2+m_B^2x^2)}{x}[4Q^2(2-x)(1+\beta)-m_u(m_{B^*}+m_B)x(1-\beta)]\,\check{\check{B}}_6(x)\\
&- e_u m_u m_B^2\frac{1}{x}\Big\{4m_B^2Q^2(2-x)x(1+\beta)\Big(\widetilde{\widetilde{C}}_6+\widetilde{\widetilde{D}}_6\Big)\\
&- (1-\beta)[m_B^3(m_{B^*}+m_B)x^3+m_B(m_{B^*}-7m_B)Q^2x-4Q^4]\,\widetilde{\widetilde{B}}_6\\
&+ 8m_B^2Q^2(2-x)x(1-\beta)\,\widetilde{\widetilde{B}}_8\Big\}(x)\\
&- 4e_s m_s m_B^4Q^2(2-x)(1-\beta)\Big(\widehat{\widehat{C}}_6-\widehat{\widehat{D}}_6\Big)(x)\\
&- e_s m_B^2\frac{1}{x}(1+\beta)\Big\{4m_BQ^2(Q^2+m_B^2x^2)(2-x)\,\widehat{\widehat{B}}_6\\
&- m_s[m_B^3(m_{B^*}+m_B)x^3+m_B(m_{B^*}-7m_B)Q^2x-4Q^4]\,\widehat{\widehat{B}}_6\\
&- 8m_s m_B^2Q^2(2-x)x\,\widehat{\widehat{B}}_8\Big\}(x)
\end{aligned}
$$

$$
\begin{aligned}
\rho_{42}^{\Sigma^{*+}}(x) &= -e_u m_B^3\frac{1}{2x}\Big\{2(1+\beta)\Big[8Q^2\,\check{\check{B}}_6-xQ^2\Big(5\,\check{\check{B}}_6-6\,\check{\check{B}}_8\Big)+m_B(m_{B^*}+m_B)x^2\Big(\check{\check{B}}_6-3\,\check{\check{B}}_8\Big)\Big]\\
&+ x(1-\beta)\Big[2[m_B(m_{B^*}+m_B)x-2Q^2]\Big(\check{\check{C}}_6+\check{\check{D}}_6\Big)-m_u(m_{B^*}+m_B)\,\check{\check{C}}_6\Big]\Big\}(x)\\
&+ e_u m_B^2\frac{1}{2x}\Big\{(1+\beta)\Big[(m_{B^*}+m_B)Q^2\,\widetilde{\widetilde{B}}_6-m_B[m_B(m_{B^*}+m_B)x-4Q^2]x\Big(\widetilde{\widetilde{B}}_6-2\,\widetilde{\widetilde{B}}_8\Big)\\
&- 2m_u m_B(m_{B^*}+m_B)x\Big(\widetilde{\widetilde{C}}_6+\widetilde{\widetilde{D}}_6\Big)\Big]\\
&+ (1-\beta)\Big[2m_B[m_B(m_{B^*}+m_B)x-2Q^2]x\Big(\widetilde{\widetilde{C}}_6-\widetilde{\widetilde{D}}_6\Big)\\
&- 8m_uQ^2\,\widetilde{\widetilde{B}}_6-m_u m_B(m_{B^*}+m_B)x\Big(\widetilde{\widetilde{B}}_6-4\,\widetilde{\widetilde{B}}_8\Big)\Big]\Big\}(x)\\
&- e_s m_B^3(m_{B^*}+m_B)\frac{1}{2x}\Big\{2x(1-\beta)\Big[m_Bx\Big(\widehat{\widehat{C}}_6+\widehat{\widehat{D}}_6\Big)+m_s\Big(\widehat{\widehat{C}}_6-\widehat{\widehat{D}}_6\Big)\Big]\\
&+ (1+\beta)\Big[2m_B[m_B(m_{B^*}+m_B)x+2Q^2-2m_s(m_{B^*}+m_B)]x\,\widehat{\widehat{B}}_8\\
&+ 2Q^2[m_{B^*}+3m_B(3-x)]\,\widehat{\widehat{B}}_6+m_s[m_B(m_{B^*}+m_B)x+8Q^2]\,\widehat{\widehat{B}}_6\Big]\Big\}(x)\\
&- e_u m_B\frac{1}{2x}(1-\beta)\Big\{2m_B^3x^3(m_{B^*}+m_B)\check{C}_2+2m_B^2Q^2x^2\Big(\check{C}_4-3\check{C}_5-\check{D}_4+3\check{D}_5\Big)\\
&- 2m_BQ^2x\Big[m_B\Big(3\check{C}_2+2\check{C}_4-6\check{C}_5-2\check{D}_4+6\check{D}_5\Big)-m_{B^*}\check{C}_2\Big]\\
&- 4Q^4\check{C}_2+2[m_B^3x^3(m_{B^*}+m_B)+m_Bx(m_{B^*}-3m_B)Q^2-2Q^4]\check{D}_2\\
&+ m_u(m_{B^*}+m_B)\Big[Q^2\Big(\check{B}_2+5\check{B}_4\Big)\\
&- m_B^2x^2\Big(\check{B}_2-\check{B}_4+6\check{B}_5+12\check{B}_7-2\check{E}_1+2\check{H}_1\Big)\Big]\Big\}(x)
\end{aligned}
$$

$$
\begin{aligned}
&+ e_u m_B \frac{1}{2x}(1+\beta)\Big\{[2Q^4 - m_B^3(m_{B^*}+m_B)x^3]\Big(\check{B}_2 + 5\check{B}_4\Big) \\
&- 2m_B^2 Q^2 x^2\Big(\check{B}_2 - \check{B}_4 + 6\check{B}_5 + 12\check{B}_7 - 2\check{E}_1 + 2\check{H}_1\Big) - m_B Q^2 x\Big[m_{B^*}\Big(\check{B}_2 + 5\check{B}_4\Big) \\
&- m_B\Big(7\check{B}_2 + 11\check{B}_4 + 24\check{B}_5 + 48\check{B}_7 - 8\check{E}_1 + 8\check{H}_1\Big)\Big] \\
&+ m_u(m_{B^*}+m_B)\Big[m_B^2 x^2\Big(\check{C}_4 - 3\check{C}_5 - \check{D}_4 + 3\check{D}_5\Big) - 2Q^2\Big(\check{C}_2 + \check{D}_2\Big)\Big]\Big\}(x) \\
&+ e_u m_B \frac{1}{2x}(1-\beta)\Big\{2m_B^2 Q^2(2-x)x\Big(\widetilde{C}_4 - \widetilde{C}_5 + \widetilde{D}_4 - \widetilde{D}_5\Big) \\
&- m_u\Big[(m_{B^*}+m_B)Q^2\Big(\widetilde{B}_2 + \widetilde{B}_4\Big) + 4m_B Q^2 x\Big(\widetilde{B}_2 - \widetilde{B}_4 + 2\widetilde{B}_5\Big) \\
&- m_B^2 x^2(m_{B^*}+m_B)\Big(\widetilde{B}_2 - \widetilde{B}_4 + 2\widetilde{B}_5 + 2\widetilde{E}_1 + 2\widetilde{H}_1\Big)\Big]\Big\}(x) \\
&+ e_u m_B \frac{1}{2x}(1+\beta)\Big\{[4Q^4 - m_B^3(m_{B^*}+m_B)x^3]\Big(\widetilde{B}_2 + \widetilde{B}_4\Big) \\
&- 8m_B^2 Q^2 x^2\Big(\widetilde{B}_5 + 2\widetilde{B}_7\Big) - m_B Q^2 x\Big[m_{B^*}\Big(\widetilde{B}_2 + \widetilde{B}_4\Big) \\
&- m_B\Big(7\widetilde{B}_2 + 7\widetilde{B}_4 + 16\widetilde{B}_5 + 32\widetilde{B}_7\Big)\Big] - m_u\Big[m_B^2(m_{B^*}+m_B)x^2\Big(\widetilde{C}_4 - \widetilde{C}_5 - \widetilde{D}_4 + \widetilde{D}_5\Big) \\
&- 2m_B Q^2 x\Big(\widetilde{C}_4 + \widetilde{C}_5 - \widetilde{D}_4 - \widetilde{D}_5\Big) - 2(m_{B^*}+m_B)Q^2\Big(\widetilde{C}_2 + \widetilde{D}_2\Big)\Big]\Big\}(x) \\
&+ e_s m_B \frac{1}{2x}(1-\beta)\Big\{4m_B^2 Q^2 x\Big[2\Big(\widehat{C}_2 + \widehat{D}_2\Big) - (2-x)\Big(\widehat{C}_5 - \widehat{D}_5\Big)\Big] \\
&+ 4Q^4\Big(\widehat{C}_2 + \widehat{D}_2\Big) - m_s\Big[m_B^2 x^2(m_{B^*}+m_B)\Big(\widehat{C}_4 - \widehat{C}_5 + \widehat{D}_4 - \widehat{D}_5\Big) \\
&- 2m_B Q^2 x\Big(\widehat{C}_4 + \widehat{C}_5 + \widehat{D}_4 + \widehat{D}_5\Big) + (m_{B^*}+m_B)Q^2\Big(\widehat{C}_2 - \widehat{D}_2\Big)\Big]\Big\}(x) \\
&+ e_s m_B \frac{1}{2x}(1+\beta)\Big\{m_B^3(m_{B^*}+m_B)x^3\Big(\widehat{B}_2 + \widehat{B}_4\Big) - 2Q^4\Big(\widehat{B}_2 - 3\widehat{B}_4\Big) \\
&- 2m_B^2 Q^2 x^2\Big(\widehat{B}_2 - \widehat{B}_4 + 2\widehat{B}_5 + 4\widehat{B}_7 - 2\widehat{E}_1 + 2\widehat{H}_1\Big) \\
&+ m_B Q^2 x\Big[m_{B^*}\Big(\widehat{B}_2 + \widehat{B}_4\Big) + m_B\Big(\widehat{B}_2 + 9\widehat{B}_4 + 8\widehat{B}_5 + 16\widehat{B}_7 - 8\widehat{E}_1 + 8\widehat{H}_1\Big)\Big] \\
&- m_s\Big[(m_{B^*}+m_B)Q^2\Big(\widehat{B}_2 + \widehat{B}_4\Big) - m_B^2(m_{B^*}+m_B)x^2\Big(\widehat{B}_2 - \widehat{B}_4 + 2\widehat{B}_5 - 2\widehat{E}_1 - 2\widehat{H}_1\Big) \\
&+ 4m_B Q^2 x\Big(\widehat{B}_2 - \widehat{B}_4 + 2\widehat{B}_5\Big)\Big]\Big\}(x) \\
&- e_u m_B^3[m_B(m_{B^*}+m_B)x - 2Q^2]\int_0^{\bar{x}} dx_3\,\Big[(1-\beta)(A_1^M - V_1^M) \\
&- 3(1+\beta)T_1^M\Big](x, 1-x-x_3, x_3) \\
&+ e_u m_B^2 \frac{1}{x}\int_0^{\bar{x}} dx_1\,\Big\{(1-\beta)(m_{B^*}+m_B)Q^2(A_1^M + V_1^M) \\
&+ (1+\beta)m_B[m_B(m_{B^*}-m_B)x - 4Q^2]xT_1^M\Big\}(x_1, x, 1-x_1-x) \\
&+ e_s m_B^2 \frac{1}{x}\int_0^{\bar{x}} dx_1\,\Big\{(1-\beta)[m_{B^*} + m_B(1+2x)]Q^2(A_1^M - V_1^M)
\end{aligned}
$$

$$
\begin{aligned}
&- (1+\beta) m_B [m_B(m_{B^*}+m_B)x + 2Q^2] x T_1^M \Big\}(x_1, 1-x_1-x, x) \\
\\
\rho_{22}^{\Sigma^{*+}}(x) &= e_u m_B^2 (m_{B^*}+m_B) \frac{1}{2x} (1+\beta)\, \widetilde{\widetilde{B}}_6(x) \\
&- e_s m_B^2 (m_{B^*}+m_B) \frac{1}{2x} (1+\beta)\, \widehat{\widehat{B}}_6(x) \\
&+ e_u m_B \frac{1}{2x} \Big\{ 2(1+\beta) \Big[Q^2 \Big(\check{B}_2 + 5\check{B}_4 \Big) - m_u (m_{B^*}+m_B) \Big(\check{C}_2 + \check{D}_2 \Big) \Big] \\
&+ (1-\beta) \Big[4Q^2 \Big(\check{C}_2 + \check{D}_2 \Big) - m_u (m_{B^*}+m_B) \Big(\check{B}_2 + 5\check{B}_4 \Big) \Big] \Big\}(x) \\
&+ e_u m_B \frac{1}{2x} \Big\{ 2(1+\beta) \Big[2Q^2 \Big(\widetilde{B}_2 + \widetilde{B}_4 \Big) + m_B (m_{B^*}+m_B) x \Big(\widetilde{B}_4 + \widetilde{B}_5 + 2\widetilde{B}_7 + \widetilde{E}_1 - \widetilde{H}_1 \Big) \\
&+ m_u (m_{B^*}+m_B) \Big(\widetilde{C}_2 + \widetilde{D}_2 \Big) \Big] + (m_{B^*}+m_B)(1-\beta) \Big[2m_B x \Big(\widetilde{C}_2 - \widetilde{C}_5 - \widetilde{D}_2 - \widetilde{D}_5 \Big) \\
&- m_u \Big(\widetilde{B}_2 + \widetilde{B}_4 \Big) \Big] \Big\}(x) \\
&+ e_s m_B \frac{1}{2x} \Big\{ (1-\beta) \Big[m_B (m_{B^*}+m_B) x \Big(\widehat{C}_4 - \widehat{C}_5 - \widehat{D}_4 + \widehat{D}_5 \Big) + 4Q^2 \Big(\widehat{C}_2 + \widehat{D}_2 \Big) \\
&+ 2m_s (m_{B^*}+m_B) \Big(\widehat{C}_2 - \widehat{D}_2 \Big) \Big] \\
&- (1+\beta) \Big[2Q^2 \Big(\widehat{B}_2 - 3\widehat{B}_4 \Big) - 2m_B (m_{B^*}+m_B) x \Big(\widehat{B}_2 + \widehat{B}_4 + 2\widehat{B}_5 + 4\widehat{B}_7 \Big) \\
&+ m_s (m_{B^*}+m_B) \Big(\widehat{B}_2 + \widehat{B}_4 \Big) \Big] \Big\}(x) \\
&+ e_u m_B (1+\beta) \int_0^{\bar{x}} dx_3 \Big\{ [m_B (m_{B^*}+m_B) x - 2Q^2] (P_1 + S_1 + 3T_1 - 6T_3) \\
&- m_u (m_{B^*}+m_B)(A_1 + 2A_3 - V_1 + 2V_3) \Big\}(x, 1-x-x_3, x_3) \\
&- e_u m_B (1-\beta) \int_0^{\bar{x}} dx_3 \Big\{ [m_B (m_{B^*}+m_B) x - 2Q^2] (A_1 + 2A_3 - V_1 + 2V_3) \\
&+ m_u (m_{B^*}+m_B)(P_1 + S_1 + 3T_1 - 6T_3) \Big\}(x, 1-x-x_3, x_3) \\
&- e_u m_B (1+\beta) \int_0^{\bar{x}} dx_1 \Big[4Q^2 (T_1 - 2T_3) - m_B (m_{B^*}+m_B) x (P_1 + S_1 + T_1 - 2T_3) \\
&- m_u (m_{B^*}+m_B)(A_1 + A_3 - V_1 + V_3) \Big](x_1, x, 1-x_1-x) \\
&- e_u \frac{1}{x} (1-\beta) \int_0^{\bar{x}} dx_1 \Big\{ - m_B^2 (m_{B^*}+m_B)(A_1^M + V_1^M) \\
&- Q^2 \Big[(m_{B^*}+m_B)(A_1 + V_1) - 2m_B x (A_3 - V_3) \Big] \\
&- m_u m_B (m_{B^*}+m_B) x (P_1 - S_1 + T_1) \Big\}(x_1, x, 1-x_1-x) \\
&- e_s m_B (1+\beta) \int_0^{\bar{x}} dx_1 \Big[2Q^2 (P_1 + S_1 + T_1 - 2T_3) - m_B (m_{B^*}+m_B) x (P_1 + S_1 - T_1 + 2T_3) \\
&+ m_s (m_{B^*}+m_B)(P_1 - S_1 - T_1) \Big](x_1, 1-x_1-x, x)
\end{aligned}
$$

$$
\begin{aligned}
&- e_s m_B(1+\beta)\int_0^{\bar{x}} dx_1 \Big[2Q^2(P_1+S_1+T_1-2T_3) - m_B(m_{B^*}+m_B)x(P_1+S_1-T_1+2T_3) \\
&+ m_s(m_{B^*}+m_B)(P_1-S_1-T_1)\Big](x_1,1-x_1-x,x) \\
&+ e_s m_B\frac{1}{x}(1-\beta)\int_0^{\bar{x}} dx_1 \Big\{m_B^2(m_{B^*}+m_B)(A_1^M-V_1^M) + Q^2\Big[(m_{B^*}+m_B+2xm_B)(A_1-V_1) \\
&+ 2m_B x(A_3+V_3)\Big] - m_s m_B(m_{B^*}+m_B)x(A_1+A_3+V_1-V_3)\Big\}(x_1,1-x_1-x,x)
\end{aligned}
$$

In the above expressions for ρ_{2i}, ρ_{4i} and ρ_{6i} the functions $\mathcal{F}(x_i)$ are defined in the following way:

$$
\begin{aligned}
\check{\mathcal{F}}(x_1) &= \int_1^{x_1} dx_1^{'}\int_0^{1-x_1^{'}} dx_3\,\mathcal{F}(x_1^{'},1-x_1^{'}-x_3,x_3)\ , \\
\check{\check{\mathcal{F}}}(x_1) &= \int_1^{x_1} dx_1^{'}\int_1^{x_1^{'}} dx_1^{''}\int_0^{1-x_1^{''}} dx_3\,\mathcal{F}(x_1^{''},1-x_1^{''}-x_3,x_3)\ , \\
\widetilde{\mathcal{F}}(x_2) &= \int_1^{x_2} dx_2^{'}\int_0^{1-x_2^{'}} dx_1\,\mathcal{F}(x_1,x_2^{'},1-x_1-x_2^{'})\ , \\
\widetilde{\widetilde{\mathcal{F}}}(x_2) &= \int_1^{x_2} dx_2^{'}\int_1^{x_2^{'}} dx_2^{''}\int_0^{1-x_2^{''}} dx_1\,\mathcal{F}(x_1,x_2^{''},1-x_1-x_2^{''})\ , \\
\widehat{\mathcal{F}}(x_3) &= \int_1^{x_3} dx_3^{'}\int_0^{1-x_3^{'}} dx_1\,\mathcal{F}(x_1,1-x_1-x_3^{'},x_3^{'})\ , \\
\widehat{\widehat{\mathcal{F}}}(x_3) &= \int_1^{x_3} dx_3^{'}\int_1^{x_3^{'}} dx_3^{''}\int_0^{1-x_3^{''}} dx_1\,\mathcal{F}(x_1,1-x_1-x_3^{''},x_3^{''})\ .
\end{aligned}
$$

Definitions of the functions B_i, C_i, D_i, E_1 and H_1 that appear in the expressions for $\rho_i(x)$ are given as follows:

$$
\begin{aligned}
B_2 &= T_1+T_2-2T_3\ , \\
B_4 &= T_1-T_2-2T_7\ , \\
B_5 &= -T_1+T_5+2T_8\ , \\
B_6 &= 2T_1-2T_3-2T_4+2T_5+2T_7+2T_8\ , \\
B_7 &= T_7-T_8\ , \\
B_8 &= -T_1+T_2+T_5-T_6+2T_7+2T_8\ , \\
C_2 &= V_1-V_2-V_3\ , \\
C_4 &= -2V_1+V_3+V_4+2V_5\ , \\
C_5 &= V_4-V_3\ , \\
C_6 &= -V_1+V_2+V_3+V_4+V_5-V_6\ , \\
D_2 &= -A_1+A_2-A_3\ , \\
D_4 &= -2A_1-A_3-A_4+2A_5\ ,
\end{aligned}
$$

$$
\begin{aligned}
D_5 &= A_3 - A_4 \ , \\
D_6 &= A_1 - A_2 + A_3 + A_4 - A_5 + A_6 \ , \\
E_1 &= S_1 - S_2 \ , \\
H_1 &= P_2 - P_1 \ .
\end{aligned}
$$

Figure captions

Fig. 1 The dependence of the helicity amplitude $A_{1/2}$ for the $\gamma^*\Sigma^+ \to \Sigma^{+*}$ transition on Q^2 at $M^2 = 1.6$ GeV^2, $s_0 = 3.5$ GeV^2, and at several fixed values of the auxiliary parameter β.

Fig. 2 The same as in Fig. 1, but for the helicity amplitude $S_{1/2}$.

Fig. 3 The same as in Fig. 1, but for the $\gamma^*\Sigma^- \to \Sigma^{-*}$ transition.

Fig. 4 The same as in Fig. 3, but for the helicity amplitude $S_{1/2}$.

Fig. 5 The same as in Fig. 1, but for the $\gamma^*\Sigma^0 \to \Sigma^{0*}$ transition.

Fig. 6 The same as in Fig. 5, but for the helicity amplitude $S_{1/2}$.

Fig. 7 The same as in Fig. 1, but for the $\gamma^*\Xi^- \to \Xi^{-*}$ transition, at $M^2 = 1.8$ GeV^2, $s_0 = 4.0$ GeV^2.

Fig. 8 The same as in Fig. 7, but for the helicity amplitude $S_{1/2}$.

Fig. 9 The same as in Fig. 7, but for the $\gamma^*\Xi^0 \to \Sigma^{-*}$ transition.

Fig. 10 The same as in Fig. 9, but for the helicity amplitude $S_{1/2}$.

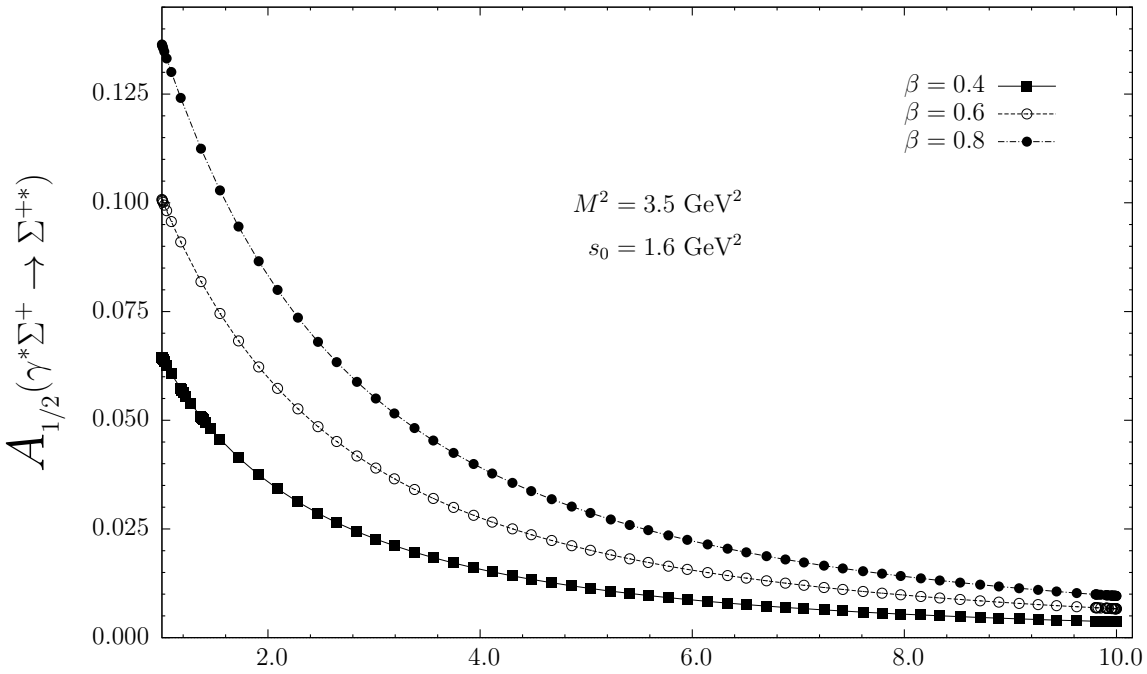

Figure 1:

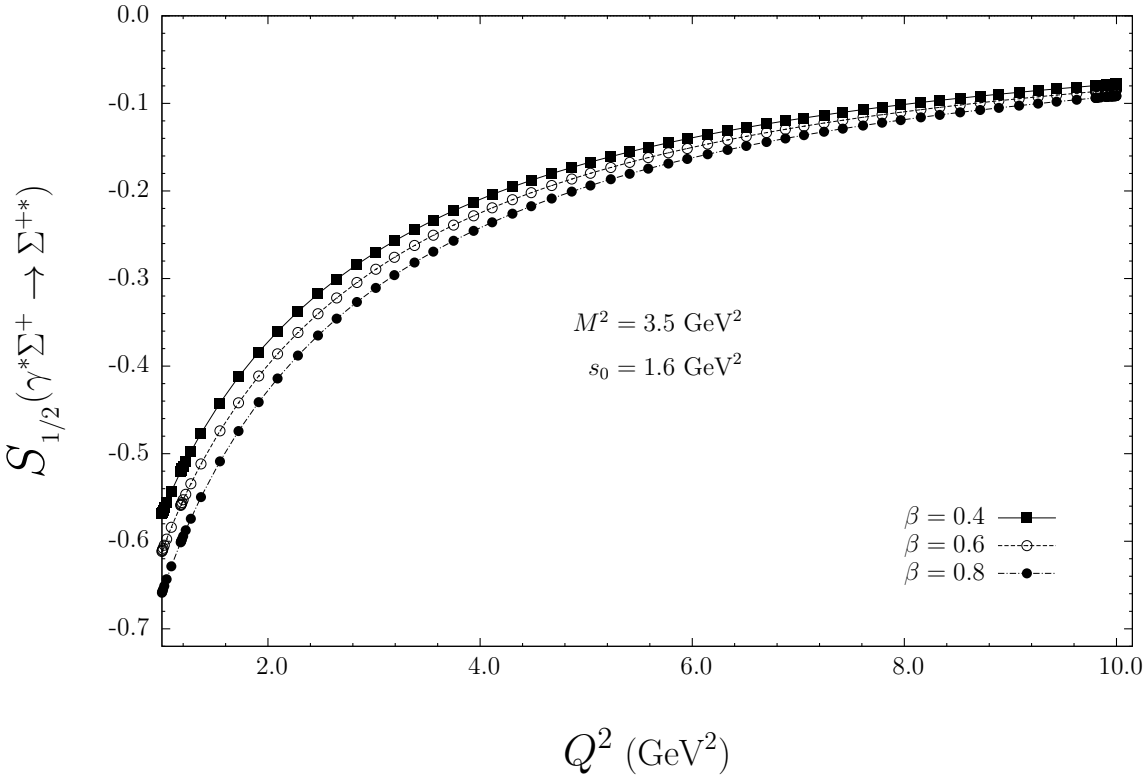

Figure 2:

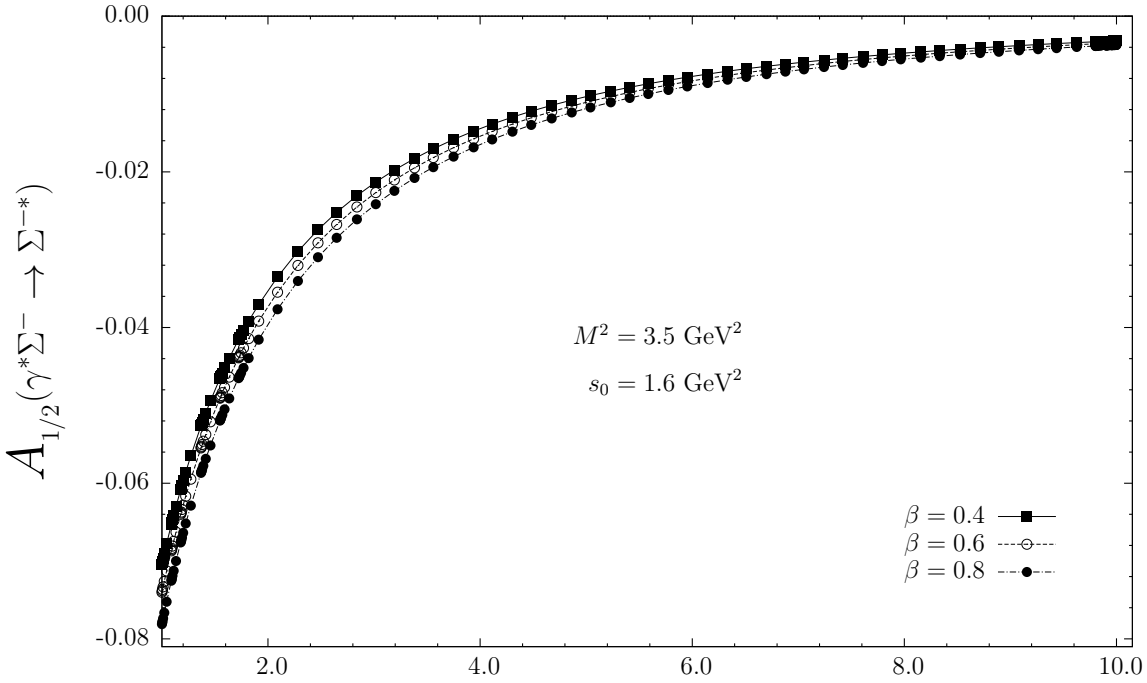

Figure 3:

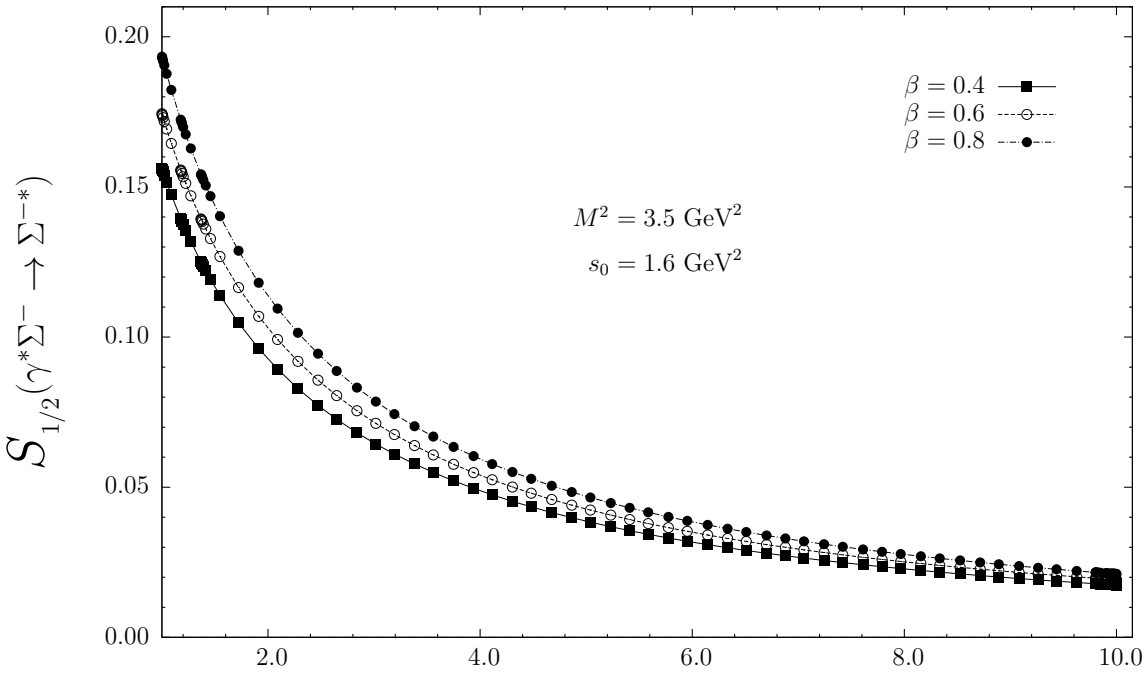

Figure 4:

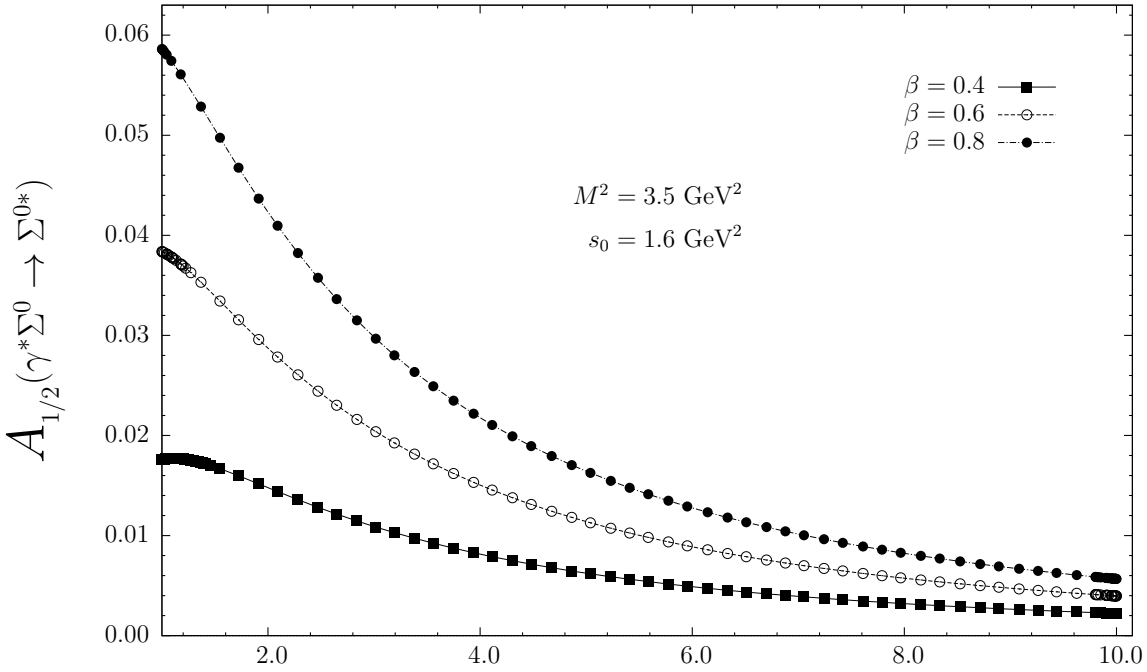

Figure 5:

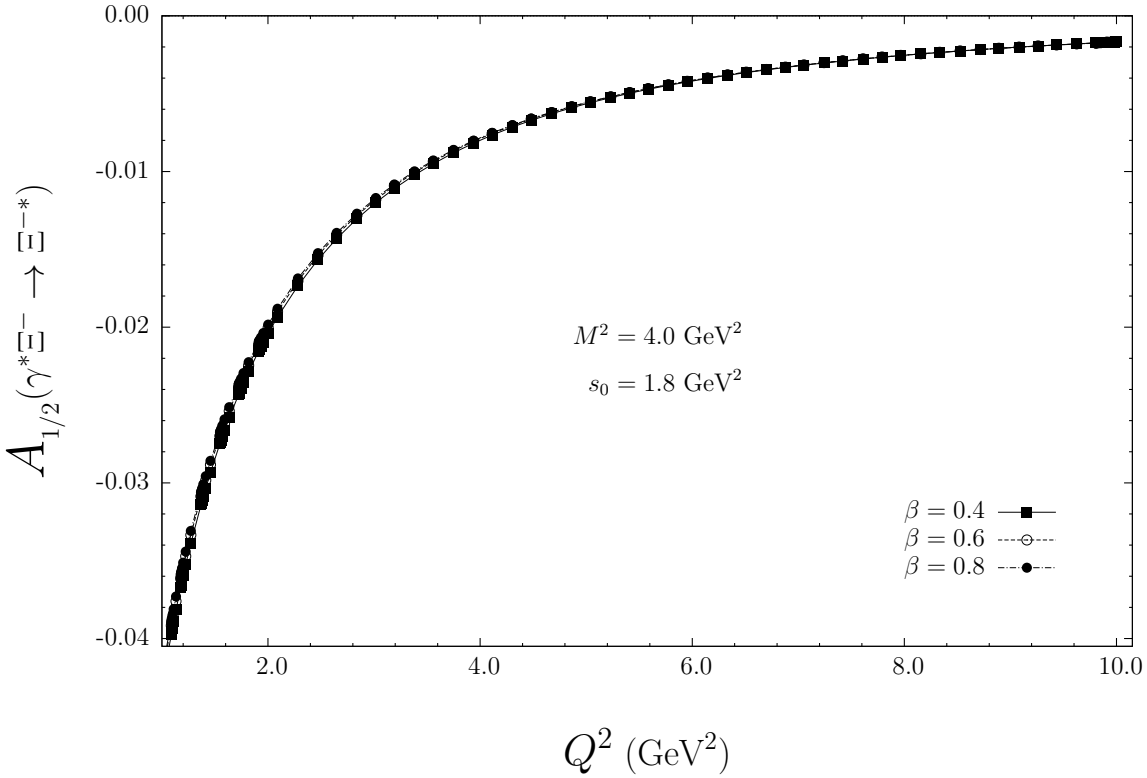

Figure 6:

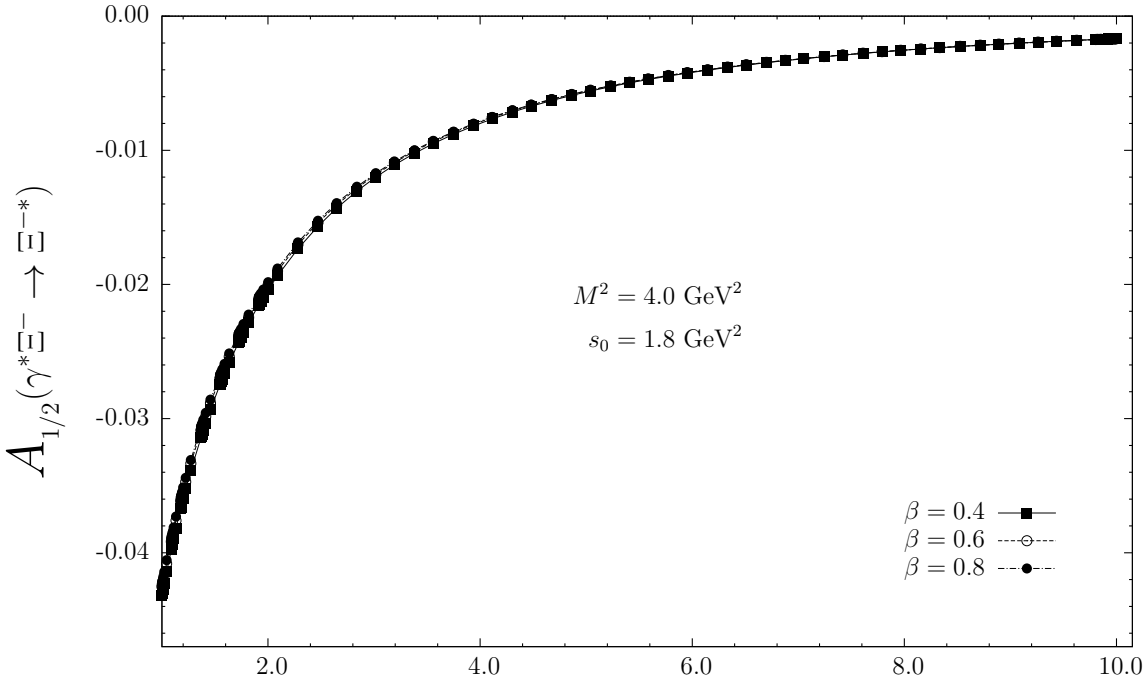

Figure 7:

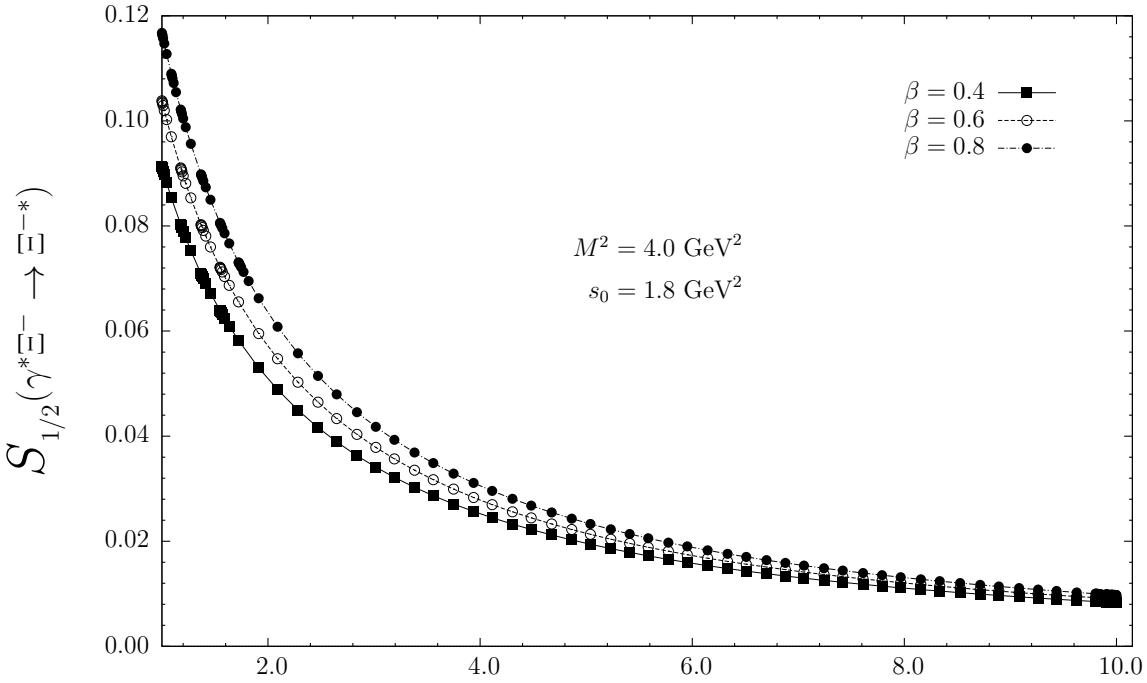

Figure 8:

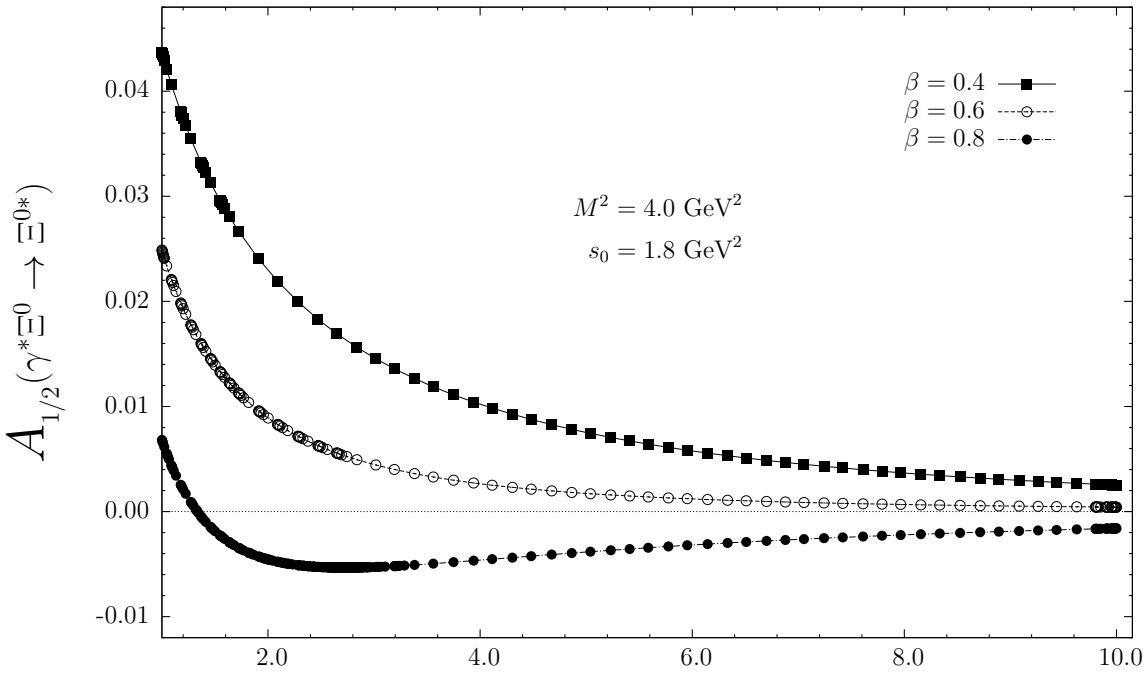

Figure 9:

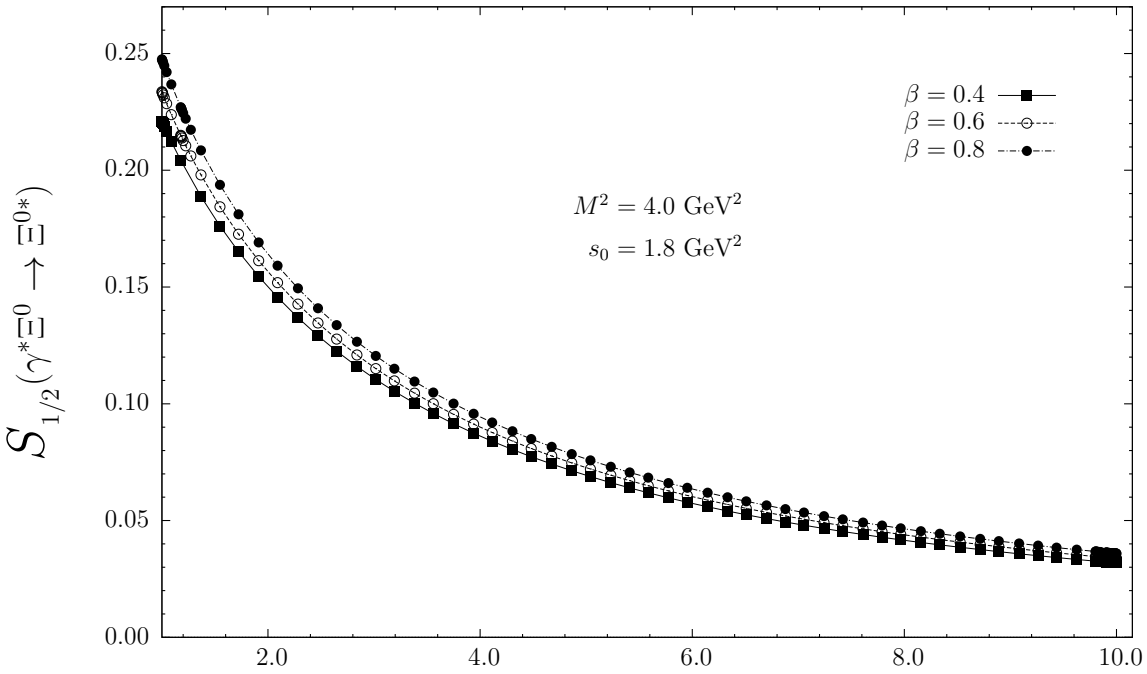

Figure 10: